X-ray Diffraction

914-Pos

Small-Angle X-Ray Scattering and Computational Modeling Reveal the Multi-Domain Assembly States of Hck in Solution

Sichun Yang[1], Lydia Blachowicz[1], Lee Makowski[2], Benoit Roux[1,2].
[1]University of Chicago, Chicago, IL, USA, [2]Argonne National Laboratory, Argonne, IL, USA.

The Src tyrosine kinases are large multi-domain enzymes [SH3-SH2-catalytic domain] involved in cellular signaling. Their ability to alternate between catalytically active (high-regulated) and inactive (down-regulated) states in response to specific signals provides a central switching mechanism in cellular transduction pathways. The activity of Src kinases is controlled by the assembly of this multi-domain enzyme. We propose an approach combining small-angle X-ray solution scattering (SAXS) with coarse-grained simulations to characterize quantitatively the multi-domain assembly states of Hck in solution. First, a basis set comprising a small number (~10) of assembly state ''classes'' is generated by clustering the configurations obtained from extensive coarse-grained simulations of Hck. Second, the average theoretical SAXS profile for each class of assembly state in the basis set is calculated by using the coarse-grained Fast-SAXS method [Yang et al, Biophys. J. 96:4449 (2009)]. Finally, the relative population of the different classes of assembly states is determined by using a Bayesian-based Monte Carlo procedure seeking to minimize the difference between the theoretical scattering pattern and SAXS data. This novel integrated approach linking experimental SAXS data and simulations is able to resolve the states of assembly of multi-domain Hck in solution under various conditions. The analysis reveals a shift in the equilibrium population of the assembly states upon the binding of various signaling peptides binding to the SH2 or SH3 domains. This integrated approach provides a new way to investigate complex multi-domain assemblies in solution.

915-Pos

X-Ray Structure of an Amyloid-Oligomer-Specific Monoclonal Antibody Fab

Hiromi Arai, Hartmut Luecke, Charles Glabe.
University of California, Irvine, Irvine, CA, USA.

The reactivity of amyloid-oligomer specific antibody, A11, towards soluble oligomer aggregates formed by proteins with varying sequences suggests that it recognizes a generic, sequence independent epitope that is shared among these soluble oligomers. This epitope appears to be associated with soluble amyloid oligomers and not with amyloid fibrils or natively-folded proteins. Currently, the detailed structure of the soluble oligomers of amyloid beta (Aβ) peptides and other amyloid-related proteins and the epitope or structural motif on soluble oligomers that these conformation-specific antibodies recognize are unknown. Co-crystallization of oligomers in complex with the antigen-binding fragments (Fab) of oligomer-specific antibodies may be a promising approach to study the structure of these oligomers due to the binding specificity of antibodies to their antigen and the crystallizability of the antigen-binding fragments (Fab) of antibodies. 48, 55, 204, and 205 (subtypes of A11) are rabbit monoclonal immunoglobulin Gs (IgGs) that show reactivity for generic oligomer epitopes. Here, the x-ray structure of 204Fab at 1.6 Å resolution is reported. The structure of the apo complementarity-determining regions (CDR) of 204Fab may provide insights into how this conformation-specific antibody recognizes Aβ oligomers. This is also the first reported structure of a rabbit Fab, and it reveals a novel interdomain disulfide bond. Crystallization trials of the Fab and ScFV (Single-chain Variable Fragments) of other oligomer-specific monoclonal antibodies and the co-crystals with oligomers are under way. If co-crystallization of the complex made of the amyloid oligomer and oligomer-specific antibodies are successful, the structural information gained from these studies may contribute to the greater understanding of the molecular mechanism of the toxicity associated with the soluble oligomers. Supported by NIH AG00538, the Cure Alzheimer Fund and a grant from the Larry L. Hillblom Foundation.

916-Pos

X-Ray Crystallography Refinement as Ewald Intended: From Drug Design to Ribosome Crystals

Michael J. Schnieders, Timothy D. Fenn, Vijay S. Pande, Axel T. Brunger.
Stanford, Stanford, CA, USA.

Precise protein-ligand complexes determined via X-ray crystallography experiments are critical for rational drug design. Here we demonstrate both improved statistical precision and greater chemical information content for a range of systems beginning with the trypsin-benzamidine complex shown below and scaling up to ribosome refinements. Keys to our method include use of the AMOEBA polarizable atomic multipole force field combined with a space group particle mesh Ewald (SG-PME) electrostatics algorithm that exploits space group symmetry to increase speed and reduce memory requirements. At high resolution (better than 1.0 Å), we achieve lower R-free statistics by using the AMOEBA electron distribution within the X-ray scattering model. At all resolutions, rigorous treatment of polarizable atomic multipole electrostatics via SG-PME improves molecular conformation and orients the water hydrogen bonding network.

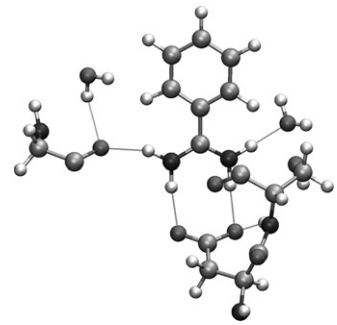

917-Pos

Pair-Distance Distribution Function P(R) of Protein Solution at Crystallographic Resolution

Xinguo Hong.
Brookhaven National Lab, Upton, NY, USA.

The pair-distance distribution function *P(r)* is a measure of the frequency of interatomic vector lengths within a protein molecule, and can provide information about the shape and intra-structure of the scattering particle. *P(r)* function has long been recognized as a smooth curve, and the oscillation at low distance is mainly due to unphysical truncation ripples in Fourier transformation.

Recently, we have developed an effective method and succeeded in collecting high-quality SAXS and WAXS of protein solutions, showing negligible radiation damage (1) (2) (3). A high resolution pair-distance distribution function, *P(r)*, of protein molecules has been obtained from the complete solution scattering curve made by combining accurate small-angle and wide-angle X-ray scattering data out to crystallographic resolution (2 Å).

Both indirect and direct Fourier transforms exhibit two distinct peaks at 1.4 Å and 5.1 Å in *P(r)*. X-ray crystallographic data demonstrate that these peaks correspond to two intramolecular distances: the average bond length between C, N and O atoms and the pitch of an α-helix, respectively. Hence some high resolution aspects of the structure and function of a protein can be investigated in solution.

Reference:
1. X. Hong and Q. Hao. 2009. Measurements of accurate x-ray scattering data of protein solutions using small stationary sample cells. Review of Scientific Instruments 80:014303.
2. X. Hong and Q. Hao. 2009. High resolution pair-distance distribution function P(r) of protein solutions. APPLIED PHYSICS LETTERS 94:083903-083903.
3. X. Hong and Q. Hao. 2009. Combining solution wide-angle X-ray scattering and crystallography: determination of molecular envelope and heavy-atom sites. Journal of Applied Crystallography 42:259-264.

Imaging & Optical Microscopy I

918-Pos

Around-the-Objective Total Internal Reflection Fluorescence Microscopy

Thomas P. Burghardt, Andrew D. Hipp, Katalin Ajtai.
Mayo Clinic Rochester, Rochester, MN, USA.

Total internal reflection fluorescence (TIRF) microscopy uses the evanescent field on the aqueous side of a glass/aqueous interface to selectively illuminate fluorophores within ~100 nm of the interface. Applications of the method include epi-illumination TIRF where the exciting light is refracted by the microscope objective to impinge on the interface at incidence angles beyond critical angle and prism based TIRF where exciting light propagates to the interface externally to the microscope optics. The former has higher background autofluorescence from the glass elements of the objective where the exciting beam is focused and the latter does not collect near-field emission from the fluorescent sample. Around-the-objective TIRF developed here creates the evanescent field by conditioning the exciting laser beam to propagate through the sub millimeter gap created by the oil immersion high numerical aperture objective and the glass coverslip. The approach eliminates background light due to the admission of the laser excitation to the microscopic optics while collecting near-field emission from the dipoles excited by the evanescent field. The aoTIRF technique was tested with 40 and 100 nanometer diameter fluorescent spheres in water that were diffusing into and out of the detection volume, BFP imaging of single 100 nm fluorescent stationary spheres adsorbed to the glass substrate of the interface, and imaging of cardiac papillary muscle fibers with exchanged GFP tagged myosin ventricular RLC. Results confirm that the evanescent field has penetration depth of ~50 nm, that the background autofluorescence from the

objective glass is significantly reduced, and that the technique is useful for imaging biological samples. Supported by NIH NIAMS R01AR049277.

919-Pos

Microscope Objective Based Surface Plasmon Resonance Imaging of Cell-Substrate Contacts

Alexander W. Peterson[1], Michael Halter[1], Alessandro Tona[2], Kiran Bhadriraju[2], Anne L. Plant[1].
[1]National Institute of Standards and Technology, Gaithersburg, MD, USA, [2]SAIC, Arlington, VA, USA.

Assembly of a high numerical objective platform for surface plasmon resonance imaging (SPRI) was used to investigate a high resolution diffraction limited refractive index image of cell-substrate contacts. SPRI is a highly sensitive biochemical surface sensor measurement technique that has only recently been applied to the field of cell-biology. The nature of the refractive index measurement made at the cell-surface interface is investigated. We present SPRI measurements of several different cell types as well as multimode image comparisons with fluorescence and transmission mode microscopies to scrutinize the signal composition of the SPRI refractive index signal. While the primary correlation of the SPRI signal appears to be the cellular membrane distance to substrate, depending on the cell type, cell focal contacts, and cellular organelles can also contribute to subcellular refractive index changes at the cell-substrate interface.

920-Pos

A Comparison of Objective Lenses for Multiphoton Microscopy: Improved Epifluorescence Collection from Turbid Samples

Avtar Singh, Jesse D. McMullen, Warren R. Zipfel.
Cornell University, Ithaca, NY, USA.

Over the past two decades, multiphoton microscopy (MPM) has launched a revolution in high-resolution *in vivo* imaging with its combination of molecular contrast, optical sectioning and depth penetration. However, as with other optical microscopies, the imaging depth of MPM is ultimately limited by the scattering of both excitation light and emitted fluorescence. Since multiphoton excitation is largely confined to a diffraction-limited focal volume, MPM can theoretically utilize any fluorescence as signal and most collection schemes seek to collect as many photons as possible. The collected fraction depends on the choice of objective lens and the design of the post-objective light collection path, as well as the optical properties of the specimen. In particular, this fraction decreases significantly in turbid samples. Recently, there has been a concerted effort by lens manufacturers to develop objective lenses that are specially tailored for MPM and aim to collect as much scattered light as possible. In order to assess the advancements made by this ''second generation'' of MP objectives, we directly measure the collected fraction from a sample consisting of a fluorescein layer below a solution of scattering microspheres. Trans- and epi-fluorescence are collected in separate channels to give a relative measure of the collected fraction and the dependence on sample scattering is compared for five different lenses. We also observe that the angular divergence of the light cone exiting the objective back increases with sample scattering- a practical detail that has implications on design of collection pathways.

921-Pos

Pixel Multiplexing for Simultaneous High Resolution High Speed Image Capture

Gil Bub, Matthias Tecza, Michiel Helmes, Peter Lee, Peter Kohl.
University of Oxford, Oxford, United Kingdom.

We introduce a imaging modality that works by transiently masking image-subregions during a single exposure of a CCD frame. By offsetting subregion exposure time, temporal information is embedded within each stored frame, allowing simultaneous acquisition of a full high spatial resolution image and a high-speed image sequence without increasing bandwidth. The technique is demonstrated by imaging calcium transients in heart cells at 250 Hz with a 10 Hz megapixel camera.

922-Pos

A Multifocal Two-Photon Microscopy Setup for Parallel 3D Tracking of Gold Nanorods

Bram van den Broek, Tjerk H. Oosterkamp, John van Noort.
Leiden University, Leiden, Netherlands.

We have constructed a laser scanning two-photon fluorescence microscopy setup that combines advantages of multiphoton microscopy (confocal 3D resolution, low phototoxicity to cells and tissue, low background autofluorescence) with the speed and sensitivity of widefield (epi) detection. A hexagonal pattern of 100 confocal scanning beams is created using a diffraction optical element (DOE). We scan this array in a spiral fashion, such that each spot forms a 2D Gaussian in the focal plane that partly overlaps with neighboring spots. In this way, homogeneous illumination is achieved with minimal load on the scanning mirror (see figure).

By detecting fluorescence with an EMCCD camera, we can create images with milliseconds exposure times. This allows us to obtain 3D fluorescence images of cells within 2 seconds.

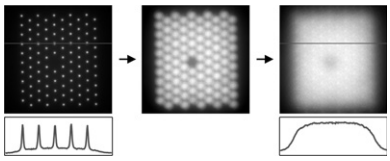

We use this setup to track the motion of multiple individual fluorescent nanoparticles. We compare the suitability of gold nanorods and quantum dots for two-photon 3D intracellular tracking. We show that the bright two-photon luminescence of gold nanorods allows video-rate tracking of single nanorods with ten nanometer accuracy. Furthermore, we explore possibilities of distinguishing closely spaced nanorods based on polarization-sensitive luminescence.

923-Pos

3D Confocal Microscope Image Enhancement by Richardson-Lucy Deconvolution Algorithm with Total Variation Regularization: Parameters Estimation

Martin Laasmaa, Marko Vendelin, Pearu Peterson.
Institute of Cybernetics at Tallinn University of Tehnology, Tallinn, Estonia.

Deconvolution is an efficient tool for enhancing both fluorescence and confocal microscopy images. Although in confocal microscopy the point spread function is rather small and images are much sharper compared to fluorescence microscopy, deconvolution can considerably improve image contrast and reduce noise.

Several deconvolution methods have been proposed for 3D microscopy. In this work, we used Richardson-Lucy (RL) iterative algorithm assuming Poisson noise. In the presence of noise, the RL algorithm does not always give a optimal solution. To reduce the effects of noise, the RL algorithm is combined with total variation regularization. As it has been shown before, total variation (TV) with a carefully chosen regularization parameter reduces intensity oscillations in homogeneous areas and helps enhance contrast on edges.

The aim of this work was to find good estimates to deconvolution algorithm parameters from the input to obtain optimal results. The test images generated from experimental data by smoothing out the noise but keeping typical structures. The analysis showed that optimal algorithm parameter Lambda is strongly correlating with the noise level. On the other hand finding the optimal parameter value is a very tedious process and so we derived formula estimating the value from the input image. The estimated Lambda turned out to give a more robust stopping criterion then the popular criterion using the threshold level for the relative change between two successive iteration steps.

We applied the deconvolution algorithm to study mitochondrial organization in rat cardiomyocytes. An open source software for deconvolving 3D images is available in http://sysbio.ioc.ee/software/.

924-Pos

A Generation-3 Programmable Array Microscope with Digital Micro-Mirror Device

Pieter A.A. De Beule, Anthony H.B. de Vries, Wouter Caarls, Donna J. Arndt-Jovin, Thomas M. Jovin.
Max-Planck-Institute for Biophysical Chemistry, Göttingen, Germany.

We present a new and improved implementation of a programmable array microscope (PAM) based on a digital micro-mirror device (DMD) spatial light modulator. The PAM provides optical sectioning in a wide-field microscope with greatly enhanced speed and sensitivity compared to conventional point-scanning confocal microscopes.[1-3] Furthermore, one obtains the ability to structure the spatial distribution and dose of illumination in the field of view according to the brightness levels observed in the sample. Such optimized light exposure (OLÉ) prolongs the available duration of imaging in time lapse experiments because of reduced photobleaching.[4]

Recent improvements in DMD reflectivity (up to 68%), format size (1080p), and speed (25 KHz binary frame rate) have enabled the design and development of a more light-efficient dual path PAM. The performance of this instrument will be described and compared to that of conventional point-scanning and spinning disk confocal microscopes.

[1] Q.S. Hanley et al., J. Microsc. **196**, 317-331 (1999); [2] R. Heintzmann et al., J. Microsc. **204**, 119-137 (2001) ; [3] Hagen et al., Micros. Res. Techniq., **72**, 431-440 (2009). [4] W. Caarls et al., manuscript in prepration